ENVIRONMENTAL STUDIES

Disease resistance in coral is mediated by distinct adaptive and plastic gene expression profiles

Nicholas J. MacKnight[1], Bradford A. Dimos[1], Kelsey M. Beavers[1], Erinn M. Muller[2], Marilyn E. Brandt[3], Laura D. Mydlarz[1]*

Infectious diseases are an increasing threat to coral reefs, resulting in altered community structure and hindering the functional contributions of disease-susceptible species. We exposed seven reef-building coral species from the Caribbean to white plague disease and determined processes involved in (i) lesion progression, (ii) within-species gene expression plasticity, and (iii) expression-level adaptation among species that lead to differences in disease risk. Gene expression networks enriched in immune genes and cytoskeletal arrangement processes were correlated to lesion progression rates. Whether or not a coral developed a lesion was mediated by plasticity in genes involved in extracellular matrix maintenance, autophagy, and apoptosis, while resistant coral species had constitutively higher expression of intracellular protein trafficking. This study offers insight into the process involved in lesion progression and within- and between-species dynamics that lead to differences in disease risk that is evident on current Caribbean reefs.

INTRODUCTION

At low prevalence, disease acts as a natural selective pressure on species and has the capacity to shape species' evolution and positively affects ecology of an environment over time (*1*, *2*). However, infectious disease outbreaks have also been observed to reduce biodiversity at a global scale (*3*, *4*), resulting in the sudden extirpation of species (*5*), and fundamentally change ecological services and productivity (*6–8*). Marine ecosystems are experiencing an increase in these disease outbreaks as a result of climate change and globalization (*9*, *10*). Marine infectious diseases are unlike terrestrial diseases, as the ocean environment is suitable for diverse microbial growth and promotes transmission through the water, and the pathogens cannot be practically removed or isolated. Therefore, disease outbreaks have become a primary threat to marine ecosystems. By understanding host susceptibility, disease scale, and pathogen virulence, we can learn from these events and work toward understanding the ecology of future marine ecosystems in a changing environment.

Coral reefs are ecologically and economically invaluable resources that have experienced gradual community biodiversity loss alongside increasingly frequent and severe disease outbreaks (*11–14*). Coral diseases are a global threat with increased prevalence and disease outbreaks reported in nearly all major ocean basins including the Caribbean, Red Sea, Indian Ocean, Indo-Pacific, and Great Barrier Reef (*15*). Coral reefs provide a unique opportunity to understand the ecology of disease dynamics, including the spatial and temporal scale of disease (*14*). An example is the historical tissue loss disease, white plague, which has gripped the Caribbean since the 1970s and is still pervasive, perhaps because of its ability to infect multiple coral hosts (*16*). Newly emerging diseases such as stony coral tissue loss disease (SCTLD) are devastating what remains of Caribbean reefs by affecting multiple species, including several species previously considered disease tolerant (*17*). Collectively, disease outbreaks are shifting the seascape toward more disease-tolerant coral species, which changes the functionality and ecological services of coral reefs.

The rise in infectious diseases emphasizes coral immunity and other disease tolerance and resistance mechanisms as an increasingly selective force in ecology. Although our understanding of immunity has increased, especially in naturally infected corals and those exposed to immune stimulators and bacteria within laboratory studies, we currently lack a sufficient understanding of how immune defenses and other cellular mechanisms vary among species. There is an urgent need to understand the difference between inducible immune responses to an active infection and the constitutive, species-specific resistance mechanisms that prevent some species from developing disease lesions. As in the example of white plague, *Montastraea cavernosa*, *Porites porites*, and *Porites astreoides* are typically more disease resistant, as demonstrated in the field and our previous study, which showed that these same species had significantly reduced relative risk of white plague disease when exposed to diseased corals (*16*). These species' resistance, however, may differ after exposure to other marine diseases, such as SCTLD, indicating that different diseases stimulate different host responses, including the host immune system (*17*).

Previous studies on coral disease and immunity have successfully identified genes induced by disease that contribute to biological processes such as apoptosis, autophagy, extracellular matrix maintenance, lipid metabolism, and protein trafficking (*18–22*). However, comparing immune responses between coral species that differ in disease resistance or susceptibility, linking specific disease phenotypes to gene expression, and determining adaptive or plastic disease resistance–associated expression patterns are understudied. By leveraging the outcome of the experimental exposure of seven coral species to white plague disease, we can identify lineage-specific expression adaptation and highly plastic genes that are linked to tangible disease phenotypes associated with coral species that are disease resistant or susceptible.

MATERIALS AND METHODS

Experimental design and sample preparation

The phenotypic response from the disease exposure experiment was originally reported by MacKnight *et al.* (*16*). Briefly, five apparently healthy parental colonies from each of seven Caribbean coral species,

[1]University of Texas at Arlington, 337 Life Science Building, Arlington, TX 76019, USA. [2]Mote Marine Laboratory, 1600 Ken Thompson Pkwy, Sarasota, FL 34236, USA. [3]University of the Virgin Islands, 2 John Brewers Bay, St. Thomas, VI 00802, USA.
*Corresponding author. Email: mydlarz@uta.edu

Orbicella faveolata, *Colpophyllia natans*, *Siderastrea siderea*, *P. astreoides*, *P. porites*, and *M. cavernosa*, were collected from Brewers Bay (18.34403°, −64.98435°), St. Thomas, Virgin Islands, USA, on 13 June 2017. Diseased *O. franksi* was targeted as the source for disease in this transmission experiment because this species is known to be consistently affected by white plague disease throughout the year and was also used as the source species for previous experiments (*23*). Both *O. franksi* colonies showing signs of tissue loss consistent with white plague disease (*n* = 3) and apparently healthy colonies (*n* = 5) were collected by separate divers and kept in isolation until the commencement of the experiment. All colonies were held in running seawater tables at the University of the Virgin Islands where they were fragmented using a sterilized table saw, acclimated for 9 days, and then placed in experimental conditions. Although five healthy parental colonies of *Orbicella annularis* were collected, one experienced mortality soon after collection and was not used in experiments. Diseased *O. franksi* corals were fragmented and monitored for lesion enlargement for 24 hours in isolation. Only fragments showing active lesion progression were used in disease treatments.

Upon commencement of the experiment (22 June 2017), coral fragments were distributed among five disease treatment and five control sterilized containers (17 liters), each equipped with individual aerators. Containers were filled with filtered seawater and placed among three outdoor shaded running seawater tables that served as water baths. Containers received water changes daily, and their locations were also randomized each day over the course of the 7-day experimental period. Each treatment container consisted of a randomly assigned healthy fragment of each of the seven tested species that were placed equal distances (approximately 7 to 8 cm) from a central diseased *O. franksi* fragment. Control containers were identically arranged, except that apparently healthy *O. franksi* were used as the central corals (Fig. 1B). When a lesion appeared on a disease-exposed coral that was previously healthy, it was monitored until 30% of the tissue was lost. If the lesion enlarged over this time period, the coral and its paired control fragment were photographed, removed, flash-frozen, and stored at −80°C. Coral fragments were classified by their treatment outcome as either "controls," "disease exposed," or "disease infected." Coral fragments exposed to apparently healthy *O. franksi* were classified as controls. Coral fragments
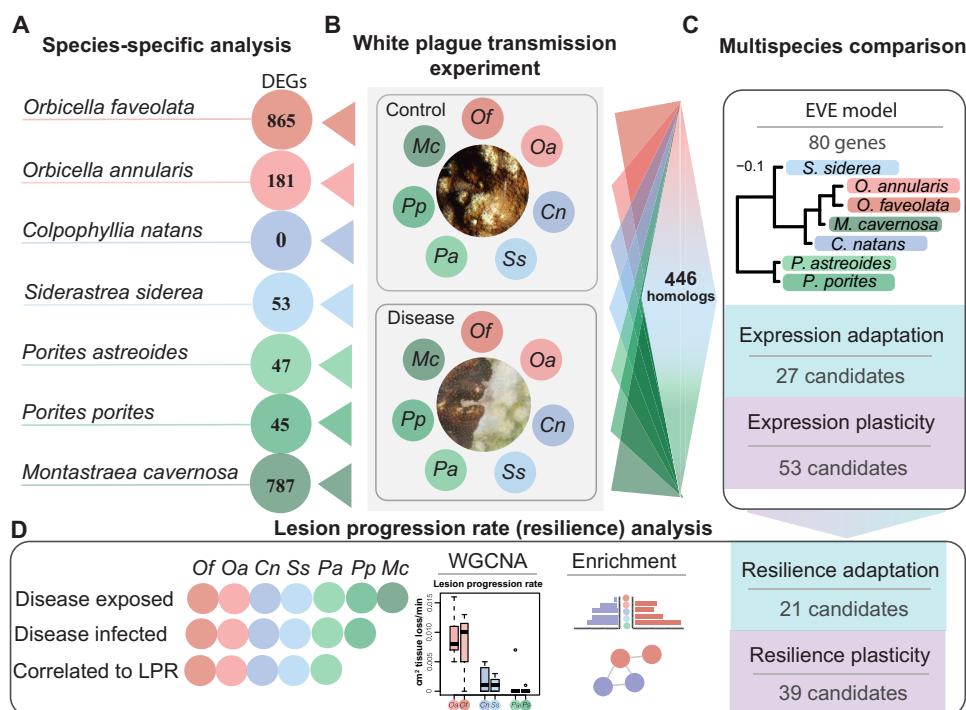
Fig. 1. Experimental design and statistical analysis overview. (**A**) RNA sequencing was performed on coral fragments of seven species (table S1), and significantly differentially expressed genes (DEGs) were identified between the control and disease treatments within each species (fig. S1). Shared DEGs between relevant species comparisons was then identified (Fig. 2). (**B**) White plague disease transmission involved apparently healthy (control) and white plague–infected *O. franksi* (disease) exposure to seven coral species. Each treatment had five replicates, and coral species were genotypically paired between treatments. (**C**) Pooling all annotated genes among the seven species identified 446 genes shared across all coral species. The expression of these genes and the phylogenetic divergence (fig. S3) of the coral species was integrated into the expression variance and evolution (EVE) model (Fig. 4). This delineated when a gene had an expression pattern that was lineage specific and a candidate for expression-level adaptation or when a gene's expression was highly plastic, and not mediated by phylogenetic differences, but likely by the disease exposure. Distinct lineage-specific and highly plastic candidates were then correlated to either relative risk, treatment outcome, or presence in modules correlated to lesion progression rate (LPR) to determine their relevance with disease resistance or susceptibility (Fig. 5 and fig. S4). (**D**) From the seven species exposed to disease (disease exposed), six species developed lesions, while five of those six species had gene coexpression networks correlated to lesion progression rate, a proxy for disease resilience. Gene modules correlated to lesion progression rate had enrichment of biological process determined within each species (fig. S2) and also among all species (Fig. 3).

exposed to disease but did not develop lesions by the end of the transmission experiment were classified as disease exposed and considered disease-resistant individuals. Coral fragments that were exposed to a diseased *O. franksi* and developed lesions that expanded through time were grouped as disease infected and considered disease-susceptible individuals. *O. faveolata* and *O. annularis* were classified as highly susceptible, *C. natans* and *S. siderea* were classified as intermediate susceptibility, and *P. porites*, *P. astreoides*, and *M. cavernosa* were classified as resistant on the basis of lesion progression rates and relative risk of disease incidence (data file S1) (*16*). The relative risk is a species-level summary statistic that represents the disease prevalence for that species, while the lesion progression rate is an individual-level statistic.

Tissue for total RNA extraction was collected from frozen coral fragments with a sterilized bone cutter and extracted with the RNAqueous™ Kit (Invitrogen). To enhance RNA integrity and yield, b-mercaptoethanol (7 µl) was added to the lysis stage and samples were lysed with a refrigerated Qiagen Tissuelyser II at 30 oscillations/s for 30 s. Elution was performed as a two-step elution (30 µl, then 30 µl) to improve RNA concentration. DNA was removed with deoxyribonuclease I (Qiagen) following the manufacturer's instructions. RNA integrity was checked with an Agilent Bioanalyzer and shipped for library prep and sequencing if the RNA integrity was above 7 with greater than a 20-ng/µl concentration. RNA was bioanalyzed again by Novogene before sequencing. Eukaryotic transcriptomic libraries were prepared through poly-A tail enrichment from total RNA at Novogene. Samples were sequenced on an Illumina HiSeq 4000 at 150 paired-end (PE) total RNA sequencing, averaging 22.5 million reads per sample (data file S2). While extraction optimization greatly improved RNA integrity and yield, not all fragments yielded sufficient RNA after multiple extraction attempts and were not sequenced as a result.

Transcriptome assembly and annotation
From the sequencer, raw reads were moved to the Mydlarz Lab's Texas system high-performance computing server. Trimmomatic v0.36 (*24*) removed reads using these parameters, which performed the following: remove adapters (ILLUMINACLIP:TruSeq3-PE. fa:2:30:10), remove leading and trailing low-quality bases (LEADING:3, TRAILING:3), scan the read with a four-base wide sliding window, cutting when the average quality per base drops below 15 (SLIDINGWINDOW:4:15), and remove reads below a 36–base pair minimum length (MINLEN:36). Trinity v2.5.1 assembled the metatranscriptomes on the Texas Advanced Computing Center's Lonestar 1-TB RAM server and then moved back to the Mydlarz Lab's server (*25*). To curate coral-only transcriptomes, metatranscriptomes were made alignable through bowtie2 v2.3.4 and then mapped with tophat against reference transcriptomes for *O. faveolata*, *P. astreoides*, and *P. porites* sourced from Fuess *et al.* (*18*) (generated for internal Mydlarz Lab use), while *S. siderea* and *C. natans* created de novo transcriptomes. *O. annularis* was mapped successfully to the *O. faveolata* reference of Fuess *et al.* (*18*). The *M. cavernosa* transcriptome was created through a genome-guided assembly from the Matz weebly 2018 *M. cavernosa* genome (*26*). Benchmarking Universal Single-Copy Orthologs analysis was used to determine the completeness of each transcriptome (*27*). Assembled sequences were annotated using UniProt-reviewed annotations, which assigned a universal gene entry ID to transcripts through BLASTX (Blast+ v2.2.27) (*28*). All gene functions discussed were sourced from the

UniProt database (*28*). Transcripts that were annotated with an e value greater than e^{-5} were removed. Transcripts from each replicate were mapped to their respective species' transcriptome using tophat v2.1.1 (*29*) and implemented through the tuxedo suite. A final count matrix was curated through HTseq v0.9.1 (*30*). One of the five *P. porites* control samples was removed from the analysis and not included in subsequent analysis because it received only 1% of the expected reads from sequencing.

Normalization and differential gene expression in response to white plague disease
EDAseq was implemented to normalize gene counts by gene length using the R package EDAseq v2.24 (*31*). Gene length–normalized expression count data from EDAseq were regularized log (rlog) normalized independently for each species, and then significantly differentially expressed genes (DEGs) were identified by comparing control and disease treatments using DEseq2 v1.30 (Fig. 1A) (*32*). Matching UniProt gene annotations of significant DEGs were identified in response to disease treatment among two subset comparisons: "susceptible species" *O. annularis* and *O. faveolata*, "phylogenetically similar and distinct susceptibility" *O. faveolata* and *M. cavernosa*, and "resistant species" *P. porites* and *M. cavernosa*. To combine genes into a subset, first, significant DEGs ($P < 0.05$) that had matching UniProt IDs between both species were identified. Raw expression of these annotated transcripts were concatenated into a subset and were EDAseq and rlog normalized together using DESeq2 v1.30. The log expression of each transcript was normalized to the base mean expression, and genes with a z score (SDs from the mean) greater than 1 were visualized, which allowed for the identification of genes that responded similarly between species to disease treatment. The presence of annotated genes for each species transcriptomes were assessed in the Gene Ontology (GO) enrichment analysis with Mann Whitney *U* test (*19*). Tests were performed to generate GO enrichment terms for the biological process, molecular function, and cellular compartment for each species with the following parameters: cluster cut height = 0.25, largest = 0.1, and smallest = 25.

Coexpression gene networks associated with lesion progression rate
Through a signed WGCNA v1.69 (weighted correlation network analysis), genes that had similar expression patterns were grouped as coexpression networks to produce gene modules (*33*). These coexpression gene network modules were assembled with a power of 18 for each species as instructed by the WGCNA user manual when working with a sample size less than 20 and a minimum module size of 100 genes. The summarized expression of these modules was then correlated to lesion progression rate as a continuous variable for each species independently. The gene expression of only disease-infected coral fragments was used in the WGCNA analysis, which included six species (*O. faveolata*, *O. annularis*, *C. natans*, *S. siderea*, *P. porites*, and *P. astreoides*) that had lesion progression rates, but only five species (*O. faveolata*, *O. annularis*, *C. natans*, *S. siderea*, and *P. porites*) had modules significantly ($P < 0.1$) correlated to lesion progression rate ($n = 16$ disease-infected coral fragments) (Fig. 1D). Genes that were correlated to lesion progression rate for each species during independent WGCNA analysis were pooled, which included eight modules consisting of 8804 unique genes positively and 13 modules consisting of 8438 unique genes

negatively correlated to lesion progression rate. The broader biological process GO enrichments were constructed using the ClueGO v2.5.7 plugin in Cytoscape v3.8.1 using UniProt entry identifiers. Genes that were uniquely positively or negatively correlated to lesion progression rates were also processed for their biological enrichment.

Multispecies comparison through an expression variance and evolution model

To create a comparable list of expressed transcripts for multispecies analysis, all transcripts with a matching UniProt ID were identified which created a list of 446 homologs (Fig. 1C and data file S3). For cases when multiple sequences were annotated to the same UniProt ID, the best matching sequence, or "top hit" as determined by the lowest e value, was retained. A species tree was generated with Species Tree from All Genes as implemented within Orthofinder2 using predicted peptides from generated transcripts with Transdecoder where lengths of the species tree represent substitutions per site (*34–37*). Single-copy orthologs with expression and gene length data were identified with Orthofinder2 (data file S4). The total identified orthologs expressed between all seven coral species was 142. Therefore, we used inferred homologs by way of matching UniProt IDs or subsequent analysis because we had a more robust list that also likely included paralogous genes that are more likely to include immune-related processes (*38*).

The list of 446 homologs were rlog normalized by species with DESeq2. This list of genes and generated species tree were input into the expression variance and evolution (EVE) model using the R package "evemodel" v0.0.0.9005 and "ape" v5.4.1 (*34*, *39*). EVE models a quantitative trait, such as the coral host's gene expression, to the coral species phylogenetic position in the tree. This formally determines whether a gene expression pattern is being mediated by potentially evolved differences between species or mediated by white plague disease exposure. The EVE model can be used for purposes such as identifying genes with high expression divergence between species as candidates for lineage-specific expression-level adaptation and genes with high expression diversity within species as candidates for expression-level plasticity (*21*, *40*). The β shared test [i.e., phylogenetic analysis of variance (ANOVA)] detected genes with increased or decreased ratios of expression divergence to diversity, represented as the β parameter. If there is stabilizing selection or no selection on the expression of a gene, then β will remain constant. This works by using an Ornstein-Uhlenbeck process of optimization to identify an ancestrally optimal expression value for each gene where variance from this optimum is represented by β. Significant deviations of β from the optimal expression value are determined through the log likelihood ratio test statistic, which follows a χ^2 distribution with one degree of freedom, and multiple testing was corrected using a false discovery rate < 0.05. If within-species gene expression variation is greater than between-species expression, then there is diversity of expression (high β), which represent candidates for expression plasticity. Gene candidates for lineage-specific expression-level adaptation are identified when within-species variation is minimal and between-species expression is divergent (low β). To confirm gene homology between species, the predicted protein-coding regions were identified and confirmed to the UniProt ID using the Pfam protein family domain (e value thresholds of 1×10^{-5}) (*41*). This analysis confirmed that (i) annotations correctly identified main protein structure and (ii) that the gene was orthologous between each species. To determine which

lineage-specific expression-level adaptation genes are associated with disease resistance, a Pearson correlation test was used to determine which lineage-specific genes had correlated expression to the species relative risk. Highly plastic genes were grouped by treatment outcome, and a Tukey post hoc test was applied to determine significant differences in gene expression between disease outcomes. Last, plastic and lineage-specific genes were identified in coexpression networks significantly correlated to lesion progression rates.

RESULTS

Transcriptome assembly

Raw sequencing reads are available for download on National Center for Biotechnology Information (NCBI; SRA accession PRJNA716052). Alignment of these reads to their respective species transcriptomes and filtering resulted in contigs expressed only in corals. A de novo transcriptome was assembled for *C. natans*. Annotation of the final transcriptomes with UniProtKB/Swiss-Prot database yielded unique annotations for 10,150 (approximately 7%) of *O. faveolata* transcripts, 22,126 (approximately 9%) of *O. annularis* transcripts, 34,828 (approximately 8.3%) of *C. natans* transcripts, 17,021 (approximately 10.1%) of *S. siderea* transcripts, 20,553 (approximately 15%) of *P. porites* transcripts, 20,546 (approximately 15%) of *P. astreoides* transcripts, and 15,214 (approximately 7%) of *M. cavernosa* transcripts.

Differential expression in response to disease treatment

Thousands of annotated genes were significantly differentially expressed (Padj < 0.05) in response to white plague exposure within each Caribbean coral species tested (fig. S2 and data file S5). The number of DEGs between treatments varied with the highest in *O. faveolata* at 865 DEGs to *C. natans* with 0 DEGs. *O. annularis* had 181 DEGs, *S. siderea* had 53 DEGs, *P. porites* with 45 DEGs, *P. astreoides* with 47 DEGs, and *M. cavernosa* had 787 DEGs. No DEGs were shared across all seven species; however, shared DEGs were identified between subsets of corals chosen because of similar or divergent phylogenic and disease susceptibility comparisons (Fig. 2). Susceptible species *O. faveolata* and *O. annularis* shared 50 DEGs. Phylogenetically similar and distinct susceptibility species, *O. faveolata* and *M. cavernosa*, had 27 shared DEGs. Resistant species *P. porites* and *M. cavernosa* shared 11 DEGs (Fig. 2 and data file S6). Across the three subset comparisons, genes that contributed to extracellular matrix maintenance and immunity were differentially expressed in response to disease exposure. Susceptible species had similar patterns of differential expression in response to disease in genes that contribute to extracellular matrix maintenance [galaxin (GXN), collagen α 2 chain, mucin-like protein, and SH3 (SRC homology 3 domain) and PX (phosphoinositide-binding structural domain)–containing protein] and immunity [coiled-coil domain–containing protein 88B, apoptosis-inducing factor 4, 4-hydroxyphenylpyruvate dioxygenase, and cartilage intermediate layer proteins (CILPs)], along with other biological processes. Phylogenetically similar species had similar differential expression of genes in response to disease exposure that contribute to extracellular matrix maintenance (matrix metalloproteinase-25 (matrix metalloproteinase inhibitors and GXN) and immunity [interferon-induced helicase C (IFIH1), CILP1, adenosine 3′,5′-monophosphate regulatory subunit type 1-α, and universal stress protein]. Resistant species had similar differential expression of genes in response to disease exposure that contribute to immunity (tyrosinase and fibrinogen-like protein A),
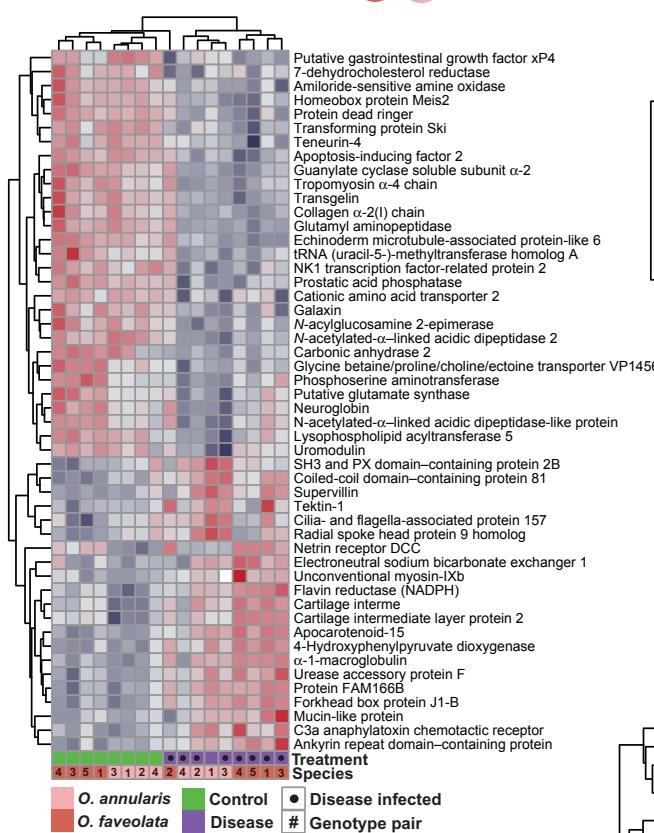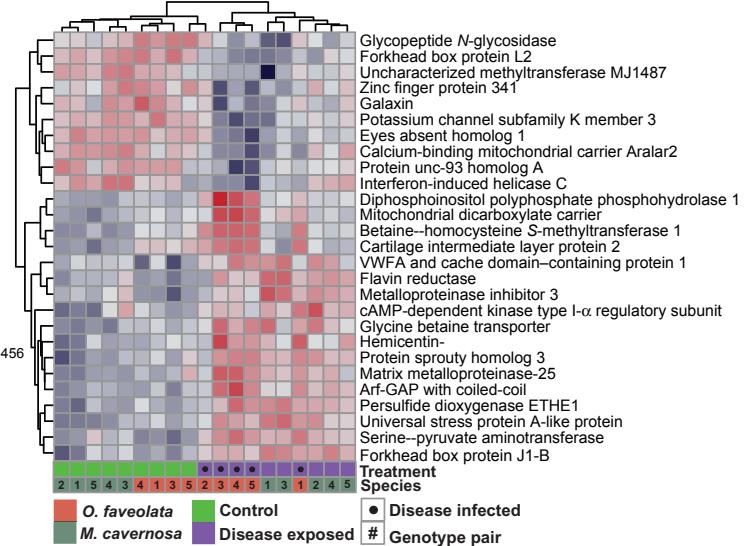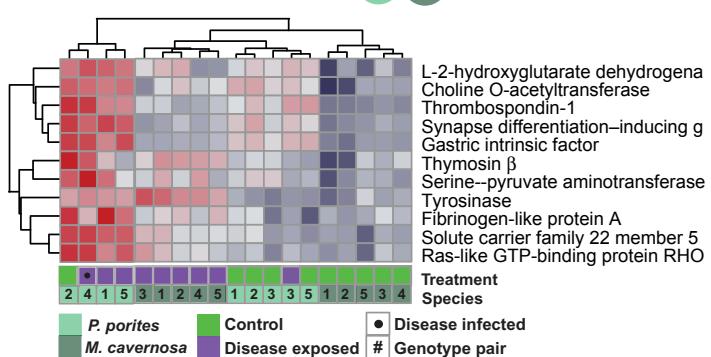
Fig. 2. Relevant comparisons of significantly DEGs. Heatmaps represent the log expression of genes normalized to the base mean of shared DEGs to demonstrate the genes that are being similarly expressed in response to treatment among relevant species comparisons. Genes were filtered to have a *z* score (SD from the mean) greater than 1 to demonstrate the genes that are more differentially expressed between control and disease treatments.

intracellular protein trafficking (Ras-like guanosine 5′-triphosphate binding protein RHO and solute carrier family 22 member 5) (Fig. 2).

Coral coexpression gene networks associated with lesion progression rate

WGCNA assigned rlog-normalized genes into modules of coexpression gene networks that were then correlated to lesion progression rate. From the six species (*O. faveolata*, *O. annularis*, *C. natans*,

S. siderea, *P. porites*, and *P. astreoides*) that displayed lesion progression rates, five species (*O. faveolata*, *O. annularis*, *C. natans*, *S. siderea*, and *P. porites*) had coexpression gene networks significantly ($P < 0.1$) correlated to lesion progression rate ($n = 16$). Significant module correlation to lesion progression rate totaled 8 modules consisting of 8804 unique genes positively correlated and 13 modules consisting of 8438 unique genes negatively correlated to lesion progression rate (Fig. 3A and fig. S2; species-specific WGCNA summary,
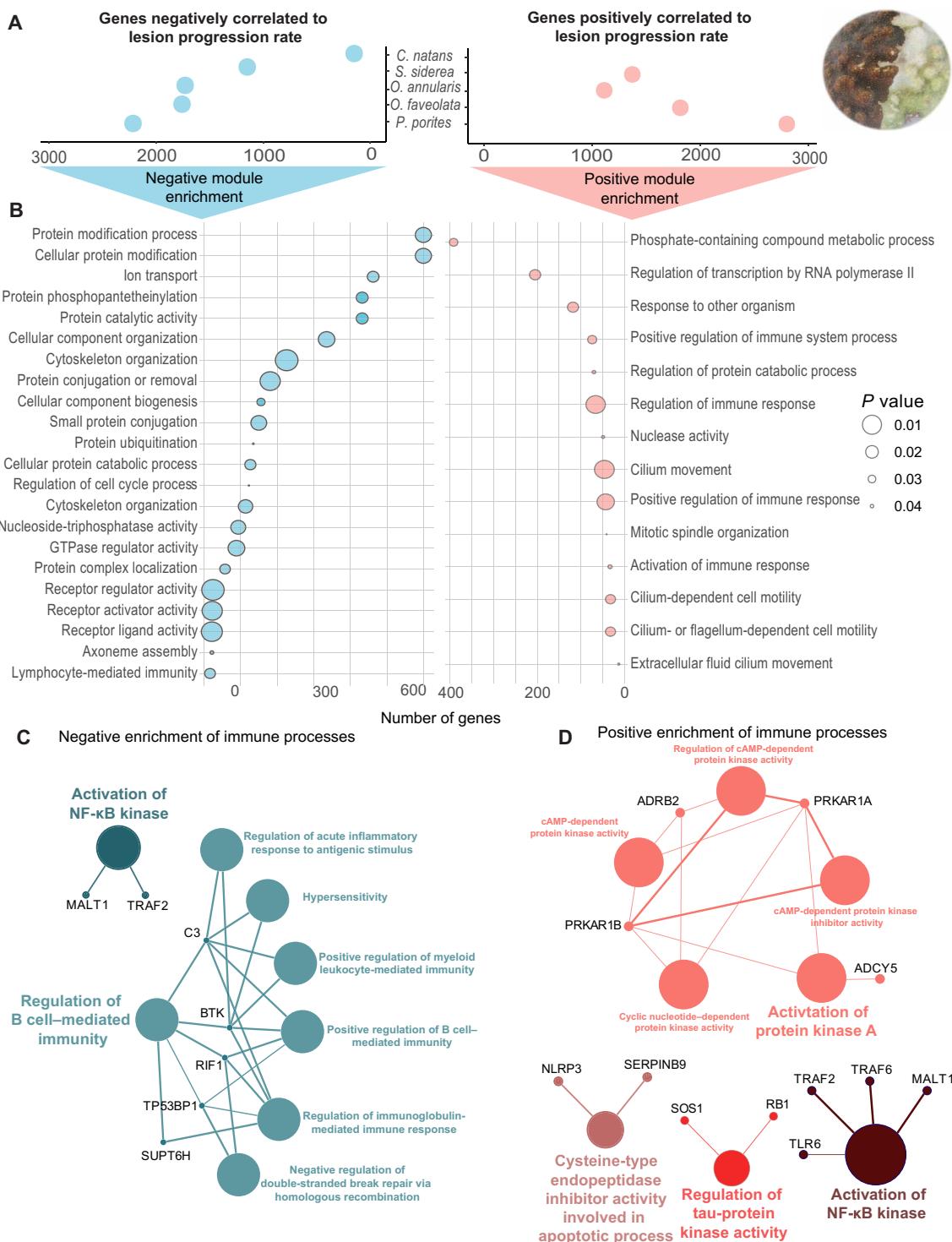
Fig. 3. Lesion progression rate among coral species. (**A**) WGCNA identified gene coexpression modules correlated to lesion progression rate for five of the seven species exposed to white plague disease. The genes in WGCNA modules that were positively correlated to lesion progression rate were pooled among species, and then the genes in WGCNA modules that were negatively correlated to lesion progression rate were pooled among species. (**B**) Enrichment of biological processes was separately determined for the pooled genes that were positively and negatively correlated to lesion progression rate. The x axis indicates the number of genes in each biological process visualized in the bubble plot. (**C** and **D**) Child terms of the parental immune-related biological processes were identified, and the genes that contributed to that enrichment were identified. Larger circles represent the enriched biological process, and smaller circles represent the genes that contribute to that enrichment.

data file S7). Module correlation to lesion progression rate was variable among species. *O. faveolata* had one module positively ($P = 0.1$ and $r = 0.8$, 1468 genes) and two modules negatively ($P = 0.02$ and $r = -0.76$, 1228 genes; $P = 0.05$ and $r = -0.68$, 563 genes) correlated to lesion progression rate. *O. annularis* had two modules positively ($P = 0.1$ and $r = 0.59$, 770 genes; $P = 0.07$ and $r = 0.67$, 381 genes) and five modules negatively ($P = 0.06$ and $r = -0.69$, 1033 genes; $P = 0.08$ and $r = -0.65$, 479 genes; $P = 0.04$ and $r = -0.72$, 132 genes; $P = 0.1$ and $r = -0.58$, 111 genes; $P = 0.01$ and $r = -0.81$, 37 genes) correlated to lesion progression rate. *S. siderea* had two modules positively ($P = 0.09$ and $r = 0.6$, 1215 genes; $P = 0.1$ and $r = 0.58$, 157 genes) and three modules negatively ($P = 0.1$ and $r = -0.53$, 580 genes; $P = 0.1$ and $r = -0.53$, 357 genes; $P = 0.01$ and $r = -0.76$, 266 genes) correlated to lesion progression rate. *C. natans* had one module positively ($P = 1 \times 10^{-4}$ and $r = 0.95$, 208 genes) and no modules negatively correlated to lesion progression rate. *P. porites* had two modules positively ($P = 0.02$ and $r = 0.7$, 2568 genes; $P = 0.1$ and $r = 0.51$, 315 genes) and three modules negatively ($P = 0.0006$ and $r = -0.8$, 1787 genes; $P = 0.07$ and $r = -0.59$, 244 genes; $P = 0.09$ and $r = -0.56$, 156 genes) correlated to lesion progression rate. One fragment of *P. astreoides* did display a lesion, but the species did not have any coexpression gene network modules significantly correlated to lesion progression rate. *M. cavernosa* did not develop lesions. Therefore, *P. astreoides* and *M. cavernosa* are omitted from this coexpression network analysis to lesion progression rate. Enrichment of terms that were uniquely positively correlated to lesion progression rate included protein modification processes and cytoskeleton arrangement–related processes (Fig. 3B). Overall, biological process enrichment that was negatively correlated to lesion progression rate included processes associated with the regulation of the immune system (Fig. 3B). Lymphocyte-mediated immunity was significantly negatively correlated to lesion progression rate and within this process were the child processes of activation of nuclear factor κB (NF-κB) kinase and regulation of B cell–mediated immunity (Fig. 3C). Four parental immune-related biological processes positively correlated to lesion progression rate had enrichment of child processes, including activation of NF-κB kinase, regulation of tau-protein kinase, activation of protein kinase A, and cysteine-type endopeptidase inhibitor activity involved in apoptotic processes (Fig. 3D).

Identifying lineage-specific and highly plastic gene expression patterns

The clustering of samples that group by species (Fig. 4A) shows that gene expression patterns are driven by coral species. To delineate phylogenetic influence compared with the influence of white plague exposure on gene expression patterns, we considered the phylogeny of species (fig. S3) in the EVE model. From the EVE model, 80 genes were significantly classified as either lineage specific or highly plastic in their expression and considered "EVE genes" (Fig. 4C and data file S8). Pfam determined 95% (76 of 80) of these genes shared similar or identical predicted protein domains among species as an inference of orthology. The remaining four were inconsistent in the predicted protein domains among species, although each are conservatively annotated accordingly as "probable" or "putative" genes and include ADAMTS (a disintegrin-like and metalloproteinase with thrombospondin motif)-like protein 1, caspase recruitment domain 15 [more likely an nod-like receptor (NLR)], putative glycosyl hydrolase ecdE, and probable 60S ribosomal protein L37-A. Within the 80 EVE genes, 27 genes had significant lineage-specific expression relative to

other species that represent gene candidates that may have contributed to species evolution (Fig. 4B). The other 53 genes were identified as highly plastic in their expression and may have expression patterns related to their exposure to disease and the response to this exposure (Fig. 4D). All 80 EVE genes are delineated by their lineage-specific expression-level adaptation or plastic expression pattern, organized by their parental GO where their log expression is visualized by color (Fig. 5).

EVE gene expression is significantly correlated to treatment outcome and relative risk

While 53 genes were significantly highly diverse in their expression among all species, 8 of these genes were significantly different among treatment outcomes (i.e., control, disease exposed, and disease infected) (Fig. 6A). This indicates that the expression of these plastic genes is mediated by the treatment conditions more strongly than by species. These eight genes were relevant in various aspects of immunity or metabolism. NF-kB suppression–related interferon regulator (Fig. 6A) and lipid metabolism through arachidonate 8-lipoxygenase (Fig. 6A) increased in expression in disease-infected fragments. Genes that significantly increased in log expression in disease-exposed coral included inflammation-related genes, tyrosine kinase receptor Tie-1, diphtheria toxin, and glycosyl hydrolase ecdE. The remaining genes had a pattern of expression that declined in expression from control to disease-infected outcomes and included wingless/integrated (WNT) signaling (nephrocystin-3), hydrolyzing glycoproteins (α L-fucosidase), folic acid metabolism, and oxireductase activity [NADPH (reduced form of nicotinamide adenine dinucleotide phosphate) pterin aldehyde reductase].

We further explored lineage-specific expression patterns to determine their association with the species relative risk of contracting white plague disease if the species is exposed. The expression patterns of one lineage-specific gene were significantly ($P = 0.048$, cor = 0.75, and df = 5) correlated to the relative risk of disease if exposed to white plague (Fig. 6B). The lipid metabolism–related, serine incorporator gene was a constitutively expressed gene that had increased expression in species with a higher relative risk of disease incidence.

Lineage-specific and highly plastic gene expression contributes to disease resilience

These 80 EVE genes were then identified in expression networks significantly correlated to lesion progression rate, a proxy for disease resilience (fig. S4 and data file S9). Thirty-seven (37) of 53 plastic genes and 23 of 27 lineage-specific genes were in one or more species' expression network that was correlated to lesion progression rate. These results indicate that both constitutive and highly plastic gene expressions are associated with lesion progression rate in coral. We further explored this to see that highly plastic genes that are commonly correlated to disease resilience in most species have a functional role that contribute to autophagy, Toll-like receptor (TLR)–to–NF-κB signaling, immune suppression, and lipid metabolism (data file S10). In addition, lineage-specific genes that were constitutively expressed in gene networks correlated to lesion progression rate were commonly related to managing cytoskeleton integrity and protein translation (fig. S4 and data file S10).

DISCUSSION

Marine diseases are increasing in scale and severity and have the capacity to reshape ecosystems (6, 14, 16, 17). By examining how
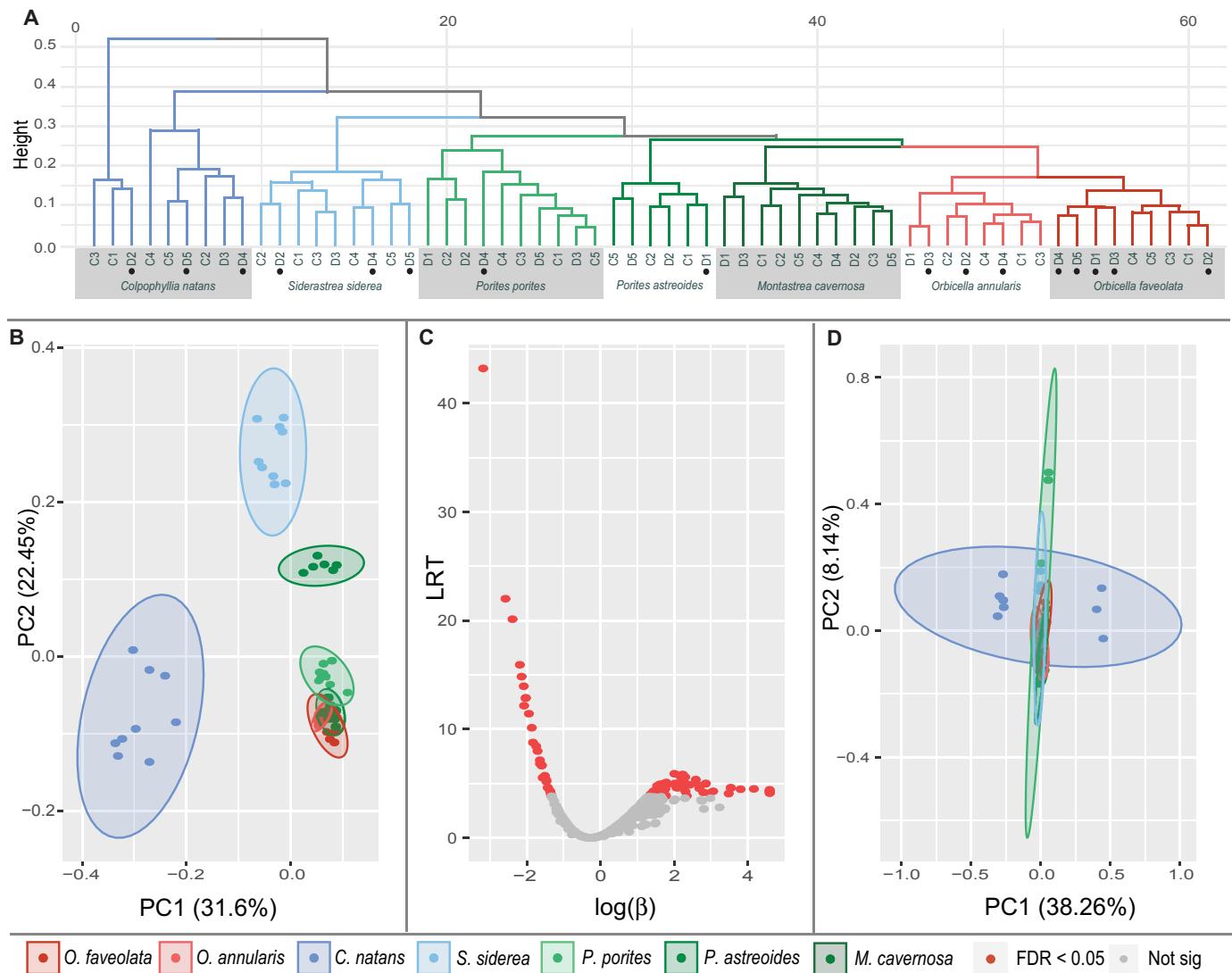
Fig. 4. EVE model. (**A**) From the gene expression of 446 shared genes, this hierarchical tree demonstrates that samples (i) separate by host species, (ii) organized by phylogenetic divergence among host species, (iii) tend to cluster by genotypic pair, regardless of treatment, and then (iv) cluster by treatment outcome if the response was influential enough (i.e., *O. faveolata*). Because response to disease is seemingly the fourth in hierarchical influence on multispecies gene expression comparisons, this warrants the need for an EVE model to isolate phylogenetic (i to iii) influential factors from the response to disease we seek to explore (iv). (**B**) EVE identified 27 genes with expression patterns that were significantly lineage-specific expression-level adaptation. (**C**) Gene expression of 446 shared genes and the phylogenetic divergence of the coral host species were integrated into the EVE model. The *y*-axis "LRT" is the likelihood ratio test result from the EVE analysis. The *x*-axis "log(β)" is a log-transformed β parameter results from the EVE analysis. (**D**) Fifty-three genes that were significantly highly plastic in their expression. FDR, false discovery rate.

disease affects coral species, we can understand the gene expression patterns that contribute to disease resistance or susceptibility and predict how disease will affect the survival and subsequent ecological contributions of a population in a changing environment. By exposing seven coral species of diverse disease susceptibility to white plague disease, the present study links lineage-specific expression-level adaptation and plasticity patterns to tangible disease phenotypes: lesion progression rate, relative risk of disease incidence, and treatment outcome. Through a combination of identifying genes with differential expression in response to disease exposure (DEGs), association with lesion progression (WGCNA), and distinction between phylogenetically and white plague exposure–mediated gene expression (EVE), we can begin to weigh the gene

expression patterns that consistently lead to either survival or lesion development during disease exposure. Our study illustrates three consistent patterns. First, in corals that developed disease lesions, immunity and cytoskeletal arrangement processes were enriched and correlated to lesion progression rate. Second, whether a coral developed lesions was mediated by plasticity in genes involved in extracellular matrix maintenance, autophagy, and apoptosis. Third, resistant species had higher levels of intracellular protein trafficking, and these processes have a lineage-specific adaptive basis to disease resistance. Together, these patterns demonstrate that the plasticity of genes that are associated with disease resistance may be evolutionarily constrained by expression-level adaptation processes.
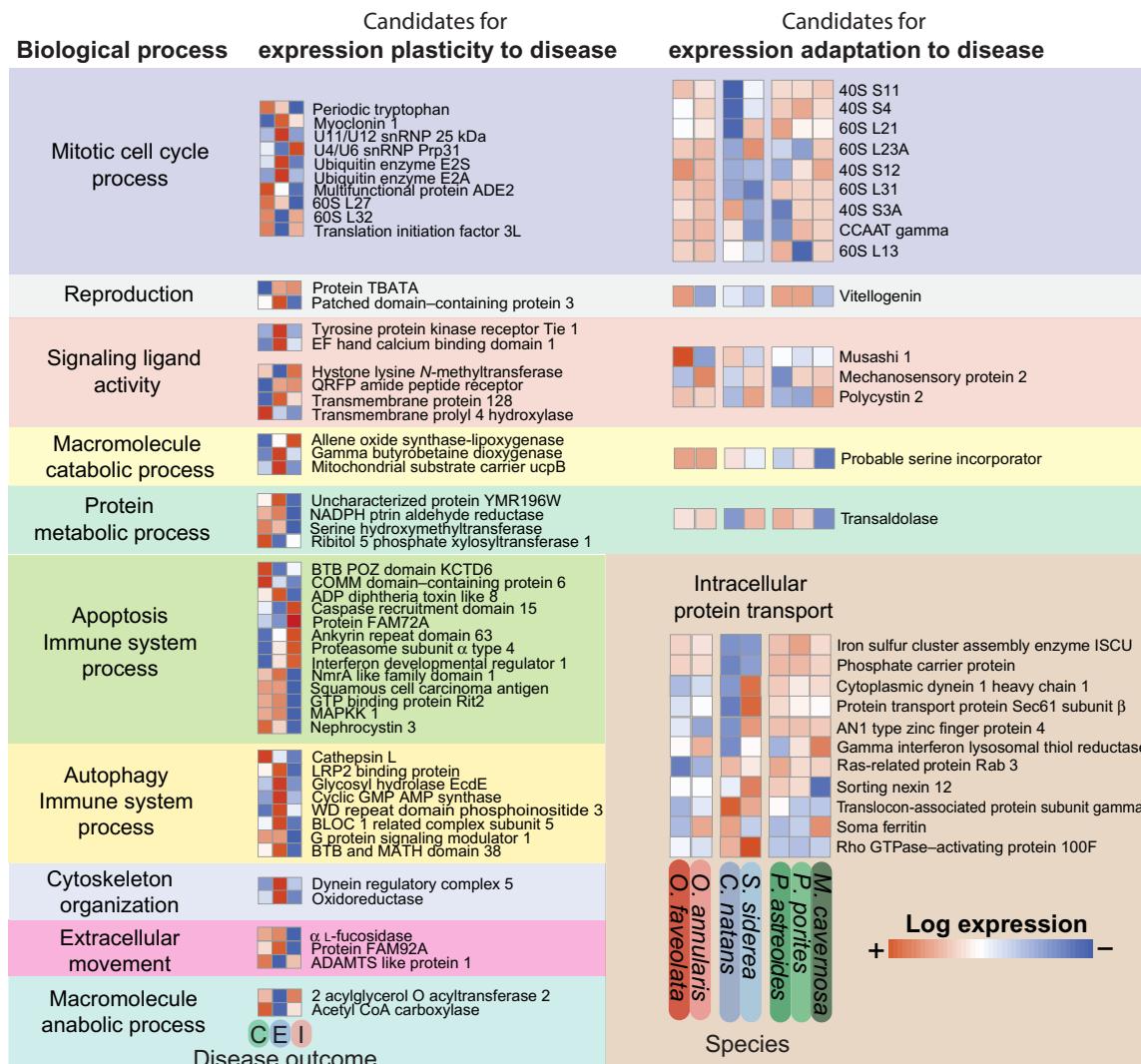
Fig. 5. Biological process enrichment of EVE genes. EVE genes were organized by the parental biological process that they contribute to as determined by Universal UniProt GO IDs. Log expression of each gene was color coordinated to indicate that red was higher expression, while blue was lower expression of a particular gene. Disease outcomes are represented by the control ("C"), disease-exposed ("E"), and disease-infected ("I") response to disease.

Lesion progression is mediated by immune signaling, cytoskeletal, and protein modification

Genes involved in the coral innate immune system were highly correlated with lesion progression rate. Coral fragments across the five species that developed lesions and had measurable lesion progression rates had higher positively correlated enrichment of immunity-associated biological processes, driven by classical immune signaling proteins, including B cell lymphoma 3 protein, tumor necrosis factor receptor–associated factor 2 (TRAF2), NACHT, LRR, and PYD domain–containing protein 3 (NLRP3), and TLR6. These proteins form core components of the coral innate immune system, which functions to detect pathogens and initiates immune responses (42). The correlation of these immune proteins with lesion progression rate indicates that as the disease progresses through coral tissue, there is activation of the immune system when the coral tissue is trying to fight infection.

Genes that were negatively correlated with lesion progression rate demonstrate a pattern of damage mitigation and slow the spread of the disease lesion. Slower lesion progression rates were mediated by genes that function in cytoskeletal organization and protein modification including cytoplasmic dynein 1 heavy chain 1 (DYNC1H1), proteasome subunit α type-7, B cell receptor–associated protein 31, serine/threonine-protein kinase mTOR (MTOR), and cathepsin B. While not considered a classical component of innate immunity, the regulation of cell structures including the cytoskeleton is an important process that promotes the cell's ability to respond and slow the progression of disease by mediating vesicle-organelle transport, extracellular matrix interactions, and cell adhesion and motility (43–45). These genes that comprise the glandular and secretory type cells, which we are now showing in this experimental work, are critical at preventing lesions from killing the organism (22). It also expands the scope of what is important and contributes to slowing the lesion progression. Some elements of NF-κB–inducing kinase activity, namely, TRAF2 and MALT1, were both positively and negatively correlated to lesion progression rates, indicating the importance of these pathways in the response to active lesions. Apoptosis has been
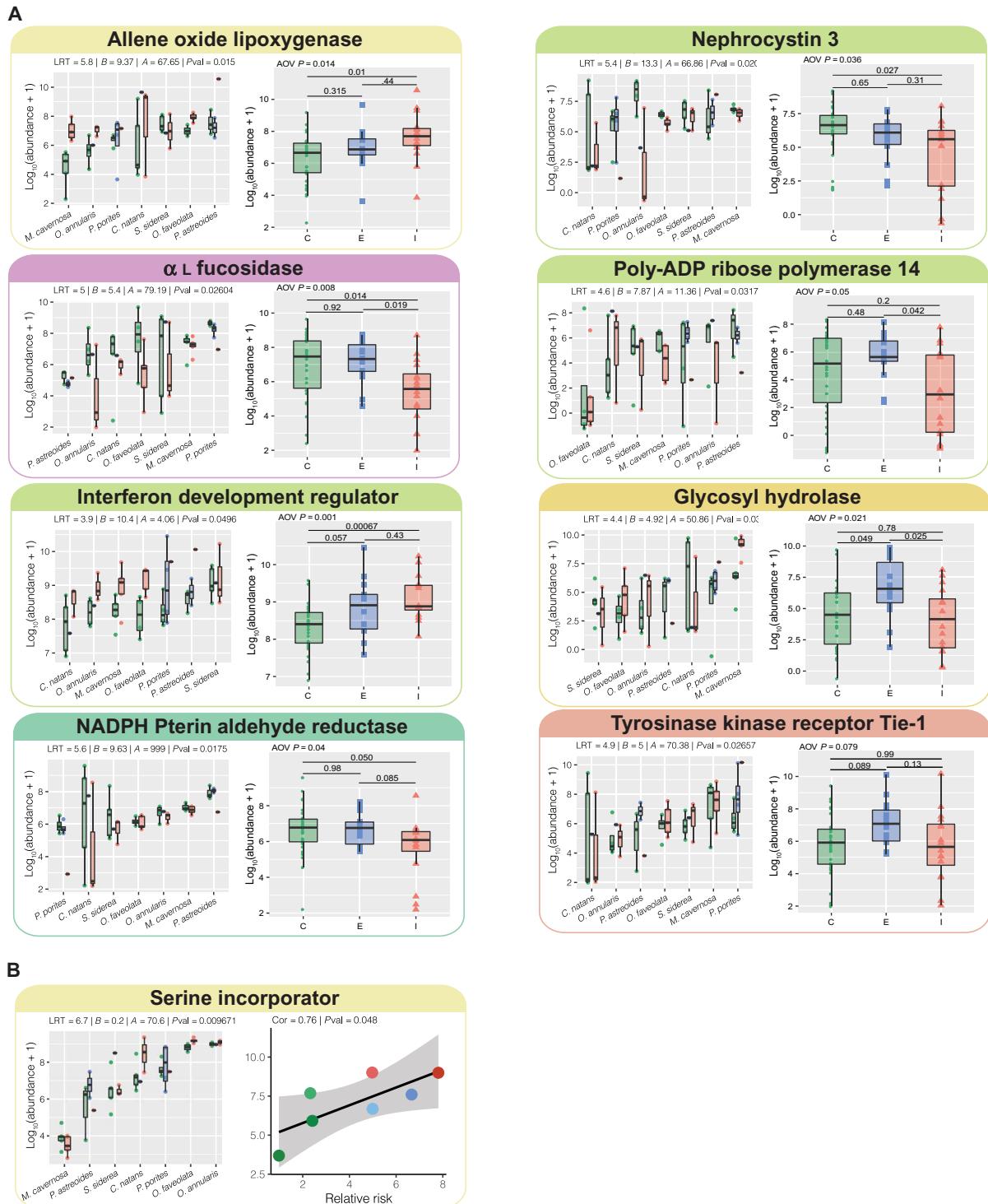
Fig. 6. Disease resistance plasticity and adaptation candidates. Gene subheader colors correspond to Fig. 5 biological processes. Within each gene panel, there is the log expression of the gene from each sample, and then the expression of that gene is pooled by treatment outcomes (A) or by species (B). LRT is the likelihood ratio test where a higher LRT value indicates a gene with a lineage-specific expression pattern. "*B*" is the β value where a higher β value indicates a gene with a highly variable expression pattern. "*A*" is the α value where a low α value indicates the genes has a stronger signal for phylogenetic recapitulation. "*P*val" determines whether the gene was significantly lineage specific or highly variable in its expression pattern. (**A**) From the 53 highly plastic genes, 8 were significantly different among treatment outcomes. "AOV *P*" indicates the ANOVA *P* value among disease outcomes. Control samples are indicated as "C" in green. Disease-exposed samples are indicated as "E" in blue. Disease-infected samples are indicated as "I" in red. ADP, adenosine 5′-diphosphate. (**B**) From the 29 lineage-specific genes, 1 was significantly correlated to relative risk of disease incidence. "Cor" is the Pearson's correlation value, and the "*P*val" is the significance of that correlation. The points on the coordination plot indicate species and colored by their spectrum of disease susceptibility.

identified as a key process used by coral to mitigate infection, but because apoptosis is irreversible, it must be controlled and mediated by the cell. Control of apoptosis has been shown to differentiate disease susceptible and resistant corals (18). TRAF2 itself may set a threshold for apoptosis and act to ubiquinate caspases (46, 47). The multiple roles for TRAF2 specifically may contribute to the sensitivity of a coral species to regulate apoptosis and fight lesions in a way that slows lesion progression or contributes to lesion advancement.

Processes associated with lesion progression rate were overwhelmingly associated with signaling the immune system, rather than downstream classical immune effectors such as antimicrobial peptides, reactive oxygen molecules, and antioxidant activities (48). These immune effectors are often posttranslationally regulated proteins that would not appear in transcriptomic datasets, or alternatively, the sampling location near the lesion or timing was not resolved enough to observe them (49). Despite this, our study shows that canonical immune signaling is involved when a disease lesion is spreading on a coral primarily in susceptible species. These same pathways were not significantly associated with lesion progression in species that had slower lesion progression rates and were more disease resistant, such as *S. siderea*.

Plasticity of autophagy, apoptosis, and extracellular matrix genes are associated with disease outcome

Gene expression plasticity in cell fate processes including the recovery pathway of autophagy or the terminal pathway of apoptosis are relevant to disease outcomes at the individual level. Namely, genes that contribute to autophagy are more highly expressed in corals fragments that were exposed to white plague but remained healthy, while the expression of genes that contribute to apoptosis is increased in fragments that developed lesions. Previous work has supported that this axis of cell fate is regulated differently in disease-resistant versus disease-susceptible corals (18, 50). Our current work shows that this is significant within species that show variability based on disease outcome. Specifically, up-regulation of lysosomal genes that promote autophagy was consistent within corals across all species that were exposed to white plague but did not develop disease lesions. Guanosine 3′,5′-monophosphate–adenosine 5′-monophosphate synthase, which activates autophagy, was also up-regulated in these disease-resistant individuals. Further autophagic activity is presented by reactive oxygen species metabolism (protein FAM72A), protein unfolding (γ-interferon–inducible lysosomal thiol reductase), and protein degradation genes [cathepsin L, low-density lipoprotein receptor-related protein 2 (LRP2)–binding proteins, and glycosyl hydrolase ecdE]. The expression of these genes was lower in the coral fragments among all species that developed disease lesions.

Conversely, genes associated with apoptosis including caspase recruitment domain 15 [nucleotide-binding oligomerization domain-containing protein 2 (NOD2)], interferon development regulator 1, allene oxide synthase-lipoxygenase, and the proteasome subunit α 4 demonstrate higher expression in fragments that developed lesions than those that remained healthy. Interferons (IFIH1) may also play a role in cytoplasmic detection of viruses and signal downstream type I interferons and proinflammatory cytokines and act as an immune regulator. Allene oxide converts arachidonic acid into oxygenated eicosanoids that act as mediators in cell stress and inflammation and results from lipid metabolic shifts (51, 52). These metabolic shifts to digest lipids have been observed during disease and bleaching, while apparently healthy coral tend to reduce lipid digestion in exchange for lipid storage (23, 53–56). Excessive levels of immune activation and inflammation can lead to apoptosis, which is further supported through the increased expression of caspase recruitment domains in disease-infected coral (18). Caspases are the effector proteins of apoptosis that are initiated through interactions with the caspase recruitment domain–containing proteins (57, 58). All of these genes that contribute to apoptosis represent patterns of highly plastic expression that indicate that immune activation and inflammation could culminate in apoptosis for coral infected with white plague disease as seen in *Acropora* white syndrome (59). Overall, we demonstrate that the genes involved in the autophagy-apoptosis axis (18, 50) show an inducible and plastic response that consistently defines resistance or lesion development across these seven diverse coral species. This advances our knowledge of cell fate decisions as a key modulator of how corals fight disease.

Disease resistance was also characterized by the induced expression of genes associated with extracellular matrix stability. Corals exposed to disease but did not develop lesions consistently down-regulated degradation of the extracellular matrix through a metalloproteinase (ADAMTS), while those coral that developed lesions down-regulated extracellular matrix–stabilizing genes (α L-fucosidase and FAM92A). Degradation proteins of the extracellular matrix are frequently up-regulated in disease-infected coral, such as astacin and gelatinase (19). Pathogens such as *Vibrio corralliilyticus* have been shown to significantly up-regulate zinc metalloproteinases to better infect coral hosts within minutes of detecting stressed coral mucus (60). The coral mucus layer is a first-line barrier defense held together by the extracellular matrix that is integral for preventing pathogen penetration and directing immune responses such as cytokine activity and wound healing (61, 62). The coral mucus layer also serves the maintenance of beneficial coral-associated microbial communities (63) and as a means to discriminate beneficial microorganisms from pathogens (64). In our previous study, we demonstrate that white plague–resistant species such as *M. cavernosa* and *Porites* spp. show a tolerance for microbial change (16), and now, we show that these species also induced plastic expression of extracellular matrix–stabilizing genes. This furthers our understanding of how host-microbiome associations can contribute to host resistance.

Extracellular matrix stability through possible mechanisms of collagen α chain, protocadherin, and hemicentin has been associated with disease-resistant individuals (20, 43). Deleted in malignant brain tumors 1 (DMBT)-1 is a putative mucosal immunity gene involved in coral microbial pattern recognition and signaling processes suspected to maintain mucosal immunity and microbial homeostasis (65–67). DMBT-1 was significantly up-regulated in disease-resistant *M. cavernosa* but significantly down-regulated in disease-susceptible *O. annularis*, further demonstrating the relevance in extracellular matrix maintenance as a plastic expression associated with disease susceptibility across species. Processes like extracellular matrix stability are proving to be very important in not only the disease response but also resistance to disease, demonstrating the valuable contributions of other aspects of coral physiology that complement or bolster the classic immune response.

Protein trafficking delineates disease resistance among species

Constitutive lineage-specific expression patterns were dominated by genes that contribute to intracellular protein trafficking, suggesting these genes are candidates for disease adaptation. Genes responsible for protein and vesicular transport had, on average, higher constitutive expression in resistant species such as *M. cavernosa*, *P. astreoides*,

and *P. porites* than in species with intermediate (*C. natans* and *S. siderea*) or high risk (*O. faveolata* and *O. annularis*) of contracting white plague. Protein trafficking is critical for mediating immune processes (*68*) such as the transport of immune vesicles, antimicrobials, or sequestration of damaged organelles (*69, 70*) and expressed higher in resistant species in this study. Namely, genes that contribute to cytoplasmic scaffolding [Iron-sulfur cluster assembly enzyme (ISCU)], cytoplasm to mitochondria transporters [phosphate carrier protein solute carrier family 25 member 3 (SLC25A3)], cytoskeletal motility (DYNC1H1), exocytosis (Ras-related protein Rab-3), and protein folding stability (AN1 zinc finger) were more highly constitutively expressed in the resistant species. Protein trafficking has demonstrated significant differential expression in response to several cellular dysfunctions such as coral disease and bleaching (*45, 71, 72*). Recent single-cell gene expression work in *Stylophora pistillata* shows that coral immune cells have up-regulated expression of vesicular trafficking, protein stability, and lysosomal genes, supporting that these processes go hand in hand (*22*). Our study shows that protein turnover and trafficking are expressed in a lineage-specific pattern that prevents corals from getting white plague disease.

Our data show consistent patterns that up-regulated protein trafficking pathways are associated with survival. This increased vesicular transport and protein trafficking in disease-resistant species such as *Porites* spp., and *M. cavernosa* may indicate better preparation to respond and fight off potential infections before lesion development occurs through inflammatory or apoptotic events. The lower expression of genes that contribute to protein trafficking in susceptible species suggests that there is an adaptive constraint that limits the susceptible species' ability to mitigate a changing environment while demonstrating a process that allows resistant corals to tolerate change. These lineage-specific expression-level disease adaptation candidates also relate to the apoptosis-autophagy axis as autophagy requires the sequestration and transport of damaged cellular components to lysosomes for turnover. A key regulator of intracellular transport that initiates autophagy and exocytosis is Ras-related protein Rab 3 (*73, 74*). This protein facilitates autophagy-related vesicle transport and is also a regulator of intracellular protein transport, which is more highly constitutively expressed in resistant coral that demonstrates why autophagy, rather than apoptosis, is successfully used in resistant coral. These resistant species have higher lineage-specific adaptive expression of the protein transport mechanisms that support this autophagic protein recycling pathway.

In conclusion, this study provides a novel framework to identify broad coral disease resistance traits. By leveraging a disease transmission experiment with seven coral species, we weigh the variable immune strategies that consistently lead to either a susceptible or resistant disease-exposure outcome that is both considerate and independent of phylogeny. The integration of disease phenotypes (disease outcome, lesion progression rate, and relative risk) into our analyses also identified processes directly involved in lesion development and progression. Considering these phenotypes, phylogeny, and gene expression broadens our understanding of processes that are relevant in mediating the holobiont's innate immune system across coral species (*16*). Faster lesion progression is widely dominated by immune signaling, while lesion arrest is promoted by the coral's modification of cytoskeletal arrangement and ability to traffic vesicles and organelles. Maintaining coral health when exposed to disease is also associated with intracellular protein trafficking mechanisms to fulfill prosurvival autophagic processes over apoptotic ones. These analyses offer insight into the evolutionary constraints of species to mitigate disease and present predictive gene-level markers and broader biological processes consistent across coral species that will shape coral reef populations in this changing environment.

SUPPLEMENTARY MATERIALS
Supplementary material for this article is available at https://science.org/doi/10.1126/sciadv.abo6153

View/request a protocol for this paper from *Bio-protocol*.

REFERENCES AND NOTES
1. D. Harvell, S. Altizer, I. M. Cattadori, L. Harrington, E. Weil, Climate change and wildlife diseases: When does the host matter the most? *Ecology* **90**, 912–920 (2009).
2. C. L. Wood, P. T. J. Johnson, A world without parasites: Exploring the hidden ecology of infection. *Front. Ecol. Environ.* **13**, 425–434 (2015).
3. C. D. Harvell, C. E. Mitchell, J. R. Ward, S. Altizer, A. P. Dobson, R. S. Ostfeld, M. D. Samuel, Climate warming and disease risks for terrestrial and marine biota. *Science* **296**, 2158–2162 (2002).
4. F. Keesing, L. K. Belden, P. Daszak, A. Dobson, C. D. Harvell, R. D. Holt, P. Hudson, A. Jolles, K. E. Jones, C. E. Mitchell, S. S. Myers, T. Bogich, R. S. Ostfeld, Impacts of biodiversity on the emergence and transmission of infectious diseases. *Nature* **468**, 647–652 (2010).
5. J. A. Pounds, M. R. Bustamante, L. A. Coloma, J. A. Consuegra, M. P. L. Fogden, P. N. Foster, E. La Marca, K. L. Masters, A. Merino-Viteri, R. Puschendorf, S. R. Ron, G. A. Sánchez-Azofeifa, C. J. Still, B. E. Young, Widespread amphibian extinctions from epidemic disease driven by global warming. *Nature* **439**, 161–167 (2006).
6. C. D. Harvell, D. Montecino-Latorre, J. M. Caldwell, J. M. Burt, K. Bosley, A. Keller, S. F. Heron, A. K. Salomon, L. Lee, O. Pontier, C. Pattengill-Semmens, J. K. Gaydos, Disease epidemic and a marine heat wave are associated with the continental-scale collapse of a pivotal predator (*Pycnopodia helianthoides*). *Sci. Adv.* **5**, eaau7042 (2019).
7. I. Hewson, J. B. Button, B. M. Gudenkauf, B. Miner, A. L. Newton, J. K. Gaydos, J. Wynne, C. L. Groves, G. Hendler, M. Murray, S. Fradkin, M. Breitbart, E. Fahsbender, K. D. Lafferty, A. M. Kilpatrick, C. M. Miner, P. Raimondi, L. Lahner, C. S. Friedman, S. Daniels, M. Haulena, J. Marliave, C. A. Burge, M. E. Eisenlord, C. D. Harvell, Densovirus associated with sea-star wasting disease and mass mortality. *Proc. Natl. Acad. Sci. U.S.A.* **111**, 17278–17283 (2014).
8. K. M. Miller, A. Teffer, S. Tucker, S. Li, A. D. Schulze, M. Trudel, F. Juanes, A. Tabata, K. H. Kaukinen, N. G. Ginther, T. J. Ming, S. J. Cooke, J. M. Hipfner, D. A. Patterson, S. G. Hinch, Infectious disease, shifting climates, and opportunistic predators: Cumulative factors potentially impacting wild salmon declines. *Evol. Appl.* **7**, 812–855 (2014).
9. J. Maynard, R. Van Hooidonk, C. M. Eakin, M. Puotinen, M. Garren, G. Williams, S. F. Heron, J. Lamb, E. Weil, B. Willis, C. D. Harvell, Projections of climate conditions that increase coral disease susceptibility and pathogen abundance and virulence. *Nat. Clim. Chang.* **5**, 688–694 (2015).
10. C. D. Harvell, K. Kim, J. M. Burkholder, R. R. Colwell, P. R. Epstein, D. J. Grimes, E. E. Hofmann, E. K. Lipp, A. D. M. E. Osterhaus, R. M. Overstreet, J. W. Porter, G. W. Smith, G. R. Vasta, Emerging marine diseases—Climate links and anthropogenic factors. *Science* **285**, 1505–1510 (1999).
11. L. M. Brander, P. Van Beukering, H. S. J. Cesar, The recreational value of coral reefs: A meta-analysis. *Ecol. Econ.* **63**, 209–218 (2007).
12. N. Pascal, M. Allenbach, A. Brathwaite, L. Burke, E. Le Port, E. Clua, Economic valuation of coral reef ecosystem service of coastal protection: A pragmatic approach. *Ecosyst. Serv.* **21**, 72–80 (2016).
13. C. A. Burge, C. Mark Eakin, C. S. Friedman, B. Froelich, P. K. Hershberger, E. E. Hofmann, L. E. Petes, K. C. Prager, E. Weil, B. L. Willis, S. E. Ford, C. D. Harvell, Climate change influences on marine infectious diseases: Implications for management and society. *Ann. Rev. Mar. Sci.* **6**, 249–277 (2014).
14. E. M. Muller, C. Sartor, N. I. Alcaraz, R. van Woesik, Spatial epidemiology of the stony-coral-tissue-loss disease in Florida. *Front. Mar. Sci.* **7**, 163 (2020).
15. P. J. Mumby, A. Hastings, H. J. Edwards, Thresholds and the resilience of Caribbean coral reefs. *Nature* **450**, 98–101 (2007).
16. N. J. MacKnight, K. Cobleigh, D. Lasseigne, A. Chaves-Fonnegra, A. Gutting, B. Dimos, J. Antoine, L. Fuess, C. Ricci, C. Butler, E. M. Muller, L. D. Mydlarz, M. Brandt, Microbial dysbiosis reflects disease resistance in diverse coral species. *Commun. Biol.* **4**, 679 (2021).
17. S. S. Meiling, E. M. Muller, D. Lasseigne, A. Rossin, A. J. Veglia, N. MacKnight, B. Dimos, N. Huntley, A. M. S. Correa, T. B. Smith, D. M. Holstein, L. D. Mydlarz, A. Apprill, M. E. Brandt, Variable species responses to experimental stony coral tissue loss disease (SCTLD) Exposure. *Front. Mar. Sci.* **8**, 670829 (2021).
18. L. E. Fuess, J. H. Pinzón, C. E. Weil, R. D. Grinshpon, L. D. Mydlarz, Life or death: Disease-tolerant coral species activate autophagy following immune challenge. *Proc. R. Soc. B Biol. Sci.* **284**, 20170771 (2017).

19. R. M. Wright, G. V. Aglyamova, E. Meyer, M. V. Matz, Gene expression associated with white syndromes in a reef building coral, *Acropora hyacinthus*. *BMC Genomics* **16**, 371 (2015).

20. N. Traylor-Knowles, M. T. Connelly, B. D. Young, K. Eaton, E. M. Muller, V. J. Paul, B. Ushijima, A. DeMerlis, M. K. Drown, A. Goncalves, N. Kron, G. A. Snyder, C. Martin, J. Rodriguez, Gene expression response to stony coral tissue loss disease transmission in *M. cavernosa* and *O. faveolata* from Florida. *Front. Mar. Sci.* **8**, 681563 (2021).

21. V. Avila-Magaña, B. Kamel, M. DeSalvo, K. Gómez-Campo, S. Enríquez, H. Kitano, R. V. Rohlfs, R. Iglesias-Prieto, M. Medina, Elucidating gene expression adaptation of phylogenetically divergent coral holobionts under heat stress. *Nat. Commun.* **12**, 5731 (2021).

22. S. Levy, A. Elek, X. Grau-Bové, S. Menéndez-Bravo, M. Iglesias, A. Tanay, T. Mass, A. Sebé-Pedrós, A stony coral cell atlas illuminates the molecular and cellular basis of coral symbiosis, calcification, and immunity. *Cell* **184**, 2973–2987.e18 (2021).

23. L. Williams, T. B. Smith, C. A. Burge, M. E. Brandt, Species-specific susceptibility to white plague disease in three common Caribbean corals. *Coral Reefs* **39**, 27–31 (2020).

24. A. M. Bolger, M. Lohse, B. Usadel, Trimmomatic: A flexible trimmer for Illumina sequence data. *Bioinformatics* **30**, 2114–2120 (2014).

25. Texas Advanced Computing Center (TACC), The University of Texas at Austin, https://www.tacc.utexas.edu/systems/lonestar6.

26. Montastrea cavernosa Genome; https://matzlab.weebly.com/data--code.html.

27. F. A. Simão, R. M. Waterhouse, P. Ioannidis, E. V. Kriventseva, E. M. Zdobnov, BUSCO: Assessing genome assembly and annotation completeness with single-copy orthologs. *Bioinformatics* **31**, 3210–3212 (2015).

28. A. Bateman, M. J. Martin, C. O'Donovan, M. Magrane, E. Alpi, R. Antunes, B. Bely, M. Bingley, C. Bonilla, R. Britto, B. Bursteinas, H. Bye-AJee, A. Cowley, A. Da Silva, M. De Giorgi, T. Dogan, F. Fazzini, L. G. Castro, L. Figueira, P. Garmiri, G. Georghiou, D. Gonzalez, E. Hatton-Ellis, W. Li, W. Liu, R. Lopez, J. Luo, Y. Lussi, A. MacDougall, A. Nightingale, B. Palka, K. Pichler, D. Poggioli, S. Pundir, L. Pureza, G. Qi, S. Rosanoff, R. Saidi, T. Sawford, A. Shypitsyna, E. Speretta, E. Turner, N. Tyagi, V. Volynkin, T. Wardell, K. Warner, X. Watkins, R. Zaru, H. Zellner, I. Xenarios, L. Bougueleret, A. Bridge, S. Poux, N. Redaschi, L. Aimo, G. ArgoudPuy, A. Auchincloss, K. Axelsen, P. Bansal, D. Baratin, M. C. Blatter, B. Boeckmann, J. Bolleman, E. Boutet, L. Breuza, C. Casal-Casas, E. De Castro, E. Coudert, B. Cuche, M. Doche, D. Dornevil, S. Duvaud, A. Estreicher, L. Famiglietti, M. Feuermann, E. Gasteiger, S. Gehant, V. Gerritsen, A. Gos, N. Gruaz-Gumowski, U. Hinz, C. Hulo, F. Jungo, G. Keller, V. Lara, P. Lemercier, D. Lieberherr, T. Lombardot, X. Martin, P. Masson, A. Morgat, T. Neto, N. Nouspikel, S. Paesano, I. Pedruzzi, S. Pilbout, M. Pozzato, M. Pruess, C. Rivoire, B. Roechert, M. Schneider, C. Sigrist, K. Sonesson, S. Staehli, A. Stutz, S. Sundaram, M. Tognolli, L. Verbregue, A. L. Veuthey, C. H. Wu, C. N. Arighi, L. Arminski, C. Chen, Y. Chen, J. S. Garavelli, H. Huang, K. Laiho, P. McGarvey, D. A. Natale, K. Ross, C. R. Vinayaka, Q. Wang, Y. Wang, L. S. Yeh, J. Zhang, UniProt: The universal protein knowledgebase. *Nucleic Acids Res.* **45**, D158–D169 (2017).

29. D. Kim, G. Pertea, C. Trapnell, H. Pimentel, R. Kelley, S. L. Salzberg, TopHat2: Accurate alignment of transcriptomes in the presence of insertions, deletions and gene fusions. *Genome Biol.* **14**, R36 (2013).

30. S. Anders, P. T. Pyl, W. Huber, HTSeq—A Python framework to work with high-throughput sequencing data. *Bioinformatics* **31**, 166–169 (2015).

31. D. Risso, K. Schwartz, G. Sherlock, S. Dudoit, GC-content normalization for RNA-seq data. *BMC Bioinformatics* **12**, 480 (2011).

32. M. I. Love, W. Huber, S. Anders, Moderated estimation of fold change and dispersion for RNA-seq data with DESeq2. *Genome Biol.* **15**, 550 (2014).

33. P. Langfelder, S. Horvath, WGCNA: An R package for weighted correlation network analysis. *BMC Bioinformatics* **9**, 559 (2008).

34. R. Rohlfs, L. Gronvold, J. Mendoza, evemodel: Expression variance evolution model. *R package version 0.0.0.9004* (2020).

35. B. J. Haas, A. Papanicolaou, M. Yassour, M. Grabherr, D. Philip, J. Bowden, M. B. Couger, D. Eccles, B. Li, M. D. Macmanes, M. Ott, J. Orvis, N. Pochet, F. Strozzi, N. Weeks, R. Westerman, T. William, C. N. Dewey, R. Henschel, R. D. Leduc, N. Friedman, A. Regev, De novo transcript sequence reconstruction from RNA-Seq using the Trinity platform for reference generation and analysis. *Nat. Protoc.* **8**, 1494–1512 (2013).

36. D. M. Emms, S. Kelly, OrthoFinder2: Fast and accurate phylogenomic orthology analysis from gene sequences. bioRxiv 466201 [**Preprint**]. 8 November 2018. https://doi.org/10.1101/466201.

37. D. M. Emms, S. Kelly, STAG: Species tree inference from all genes. bioRxiv 267914 [**Preprint**]. 19 February 2018. https://doi.org/10.1101/267914.

38. B. Dimos, M. Emery, K. Beavers, N. MacKnight, M. Brandt, J. Demuth, L. Mydlarz, Adaptive variation in homologue number within transcript families promotes expression divergence in reef-building coral. *Mol. Ecol.* **31**, 2594–2610 (2022).

39. E. Paradis, K. Schliep, ape 5.0: An environment for modern phylogenetics and evolutionary analyses in R. *Bioinformatics* **35**, 526–528 (2018).

40. M. A. Bernal, C. Schunter, R. Lehmann, D. J. Lightfoot, B. J. M. Allan, H. D. Veilleux, J. L. Rummer, P. L. Munday, T. Ravasi, Species-specific molecular responses of wild coral reef fishes during a marine heatwave. *Sci. Adv.* **6**, eaay3423 (2020).

41. A. Bateman, L. Coin, R. Durbin, R. D. Finn, V. Hollich, S. Griffiths-Jones, A. Khanna, M. Marshall, S. Moxon, E. L. L. Sonnhammer, D. J. Studholme, C. Yeats, S. R. Eddy, The Pfam protein families database. *Nucleic Acids Res.* **32**, D138–D141 (2004).

42. L. D. Mydlarz, L. Fuess, J. H. Pinzón, D. Gochfeld, Cnidarian immunity: From genomes to phenomes, 10.1007/978-3-319-31305-4_28 (1995).

43. B. D. Young, X. M. Serrano, S. M. Rosales, M. W. Miller, D. Williams, N. Traylor-Knowles, Innate immune gene expression in *Acropora palmata* is consistent despite variance in yearly disease events. *PLOS ONE* **15**, e0228514 (2020).

44. E. R. Kelley, R. S. Sleith, M. V. Matz, R. M. Wright, Gene expression associated with disease resistance and long-term growth in a reef-building coral. *R. Soc. Open Sci.* **8**, 210113 (2021).

45. C. Daniels, S. Baumgarten, L. K. Yum, C. T. MIchell, T. Bayer, C. Arif, C. Roder, E. Weil, C. R. Voolstra, Metatranscriptome analysis of the reef-building coral *Orbicella faveolata* indicates holobiont response to coral disease. *Front. Mar. Sci.* **2**, 62 (2015).

46. F. Gonzalvez, D. Lawrence, B. Yang, S. Yee, R. Pitti, S. Marsters, V. C. Pham, J. P. Stephan, J. Lill, A. Ashkenazi, TRAF2 sets a threshold for extrinsic apoptosis by tagging caspase-8 with a ubiquitin shutoff timer. *Mol. Cell* **48**, 888–899 (2012).

47. Z. P. Xia, Z. J. Chen, TRAF2: A double-edged sword? *Sci. STKE* **2005**, pe7 (2005).

48. M. G. Parisi, D. Parrinello, L. Stabili, M. Cammarata, Cnidarian immunity and the repertoire of defense mechanisms in anthozoans. *Biology* **9**, 283 (2020).

49. S. Christgen, D. E. Place, T.-D. Kanneganti, Toward targeting inflammasomes: Insights into their regulation and activation. *Cell Res.* **30**, 315–327 (2020).

50. G. Mariño, M. Niso-Santano, E. H. Baehrecke, G. Kroemer, Self-consumption: The interplay of autophagy and apoptosis. *Nat. Rev. Mol. Cell Biol.* **15**, 81–94 (2014).

51. H. Lõhelaid, T. Teder, N. Samel, Lipoxygenase-allene oxide synthase pathway in octocoral thermal stress response. *Coral Reefs* **34**, 143–154 (2015).

52. T. Teder, N. Samel, H. Lõhelaid, Distinct characteristics of the substrate binding between highly homologous catalase-related allene oxide synthase and hydroperoxide lyase. *Arch. Biochem. Biophys.* **676**, 108126 (2019).

53. S. Libro, S. T. Kaluziak, S. V. Vollmer, RNA-seq profiles of immune related genes in the staghorn coral acropora cervicornis infected with white band disease. *PLOS ONE* **8**, e81821 (2013).

54. E. P. Santoro, R. M. Borges, J. L. Espinoza, M. Freire, C. S. M. A. Messias, H. D. M. Villela, L. M. Pereira, C. L. S. Vilela, J. G. Rosado, P. M. Cardoso, P. M. Rosado, J. M. Assis, G. A. S. Duarte, G. Perna, A. S. Rosado, A. Macrae, C. L. Dupont, K. E. Nelson, M. J. Sweet, C. R. Voolstra, R. S. Peixoto, Coral microbiome manipulation elicits metabolic and genetic restructuring to mitigate heat stress and evade mortality. *Sci. Adv.* **7**, eabg3088 (2021).

55. R. A. Quinn, M. J. A. Vermeij, A. C. Hartmann, I. G. d'Auriac, S. Benler, A. Haas, S. D. Quistad, Y. W. Lim, M. Little, S. Sandin, J. E. Smith, P. C. Dorrestein, F. Rohwer, Metabolomics of reef benthic interactions reveals a bioactive lipid involved in coral defence. *Proc. R Soc. B Biol. Sci.* **283**, 20160469 (2016).

56. R. M. Wright, H. Mera, C. D. Kenkel, M. Nayfa, L. K. Bay, M. V. Matz, Positive genetic associations among fitness traits support evolvability of a reef-building coral under multiple stressors. *Glob. Chang. Biol.* **25**, 3294–3304 (2019).

57. M. S. Mohamed, M. K. Bishr, F. M. Almutairi, A. G. Ali, Inhibitors of apoptosis: Clinical implications in cancer. *Apoptosis* **22**, 1487–1509 (2017).

58. S. Shrestha, J. Tung, R. D. Grinshpon, P. Swartz, P. T. Hamilton, B. Dimos, L. Mydlarz, A. Clay Clark, Caspases from scleractinian coral show unique regulatory features. *J. Biol. Chem.* **295**, 14578–14591 (2020).

59. T. D. Ainsworth, E. C. Kvennefors, L. L. Blackall, M. Fine, O. Hoegh-Guldberg, Disease and cell death in white syndrome of Acroporid corals on the great barrier reef. *Mar. Biol.* **151**, 19–29 (2007).

60. C. Gao, M. Garren, K. Penn, V. I. Fernandez, J. R. Seymour, J. R. Thompson, J.-B. Raina, R. Stocker, Coral mucus rapidly induces chemokinesis and genome-wide transcriptional shifts toward early pathogenesis in a bacterial coral pathogen. *ISME J.* **15**, 3668–3682 (2021).

61. G. Y. Chen, G. Nuñez, Sterile inflammation: Sensing and reacting to damage. *Nat. Rev. Immunol.* **10**, 826–837 (2010).

62. K. S. Midwood, A. M. Piccinini, DAMPening inflammation by modulating TLR signalling. *Mediators Inflamm.* **2010**, 672395 (2010).

63. K. B. Ritchie, Regulation of microbial populations by coral surface mucus and mucusassociated bacteria. *Mar. Ecol. Prog. Ser.* **322**, 1–14 (2006).

64. A. Boilard, C. E. Dubé, C. Gruet, A. Mercière, A. Hernandez-Agreda, N. Derome, Defining coral bleaching as a microbial dysbiosis within the coral holobiont. *Microorganisms* **8**, 1682 (2020).

65. R. M. Wright, C. D. Kenkel, C. E. Dunn, E. N. Shilling, L. K. Bay, M. V. Matz, Intraspecific differences in molecular stress responses and coral pathobiome contribute to mortality under bacterial challenge in *Acropora millepora*. *Sci. Rep.* **7**, 2609 (2017).

66. L. E. Fuess, W. T. Mann, L. R. Jinks, V. Brinkhuis, L. D. Mydlarz, Transcriptional analyses provide new insight into the late-stage immune response of a diseased Caribbean coral. *R. Soc. Open Sci.* **5**, 172062 (2018).

67. C. Y. M. Huang, C. Zhang, D. R. Zollinger, C. Leterrier, M. N. Rasband, An αII spectrin-based cytoskeleton protects large-diameter myelinated axons from degeneration. *J. Neurosci.* **37**, 11323–11334 (2017).

68. A. Benado, Y. Nasagi-Atiya, R. Sagi-Eisenberg, Protein trafficking in immune cells. *Immunobiology* **214**, 507–525 (2009).

69. M. C. Chen, Y. M. Cheng, P. J. Sung, C. E. Kuo, L. S. Fang, Molecular identification of Rab7 (ApRab7) in *Aiptasia pulchella* and its exclusion from phagosomes harboring zooxanthellae. *Biochem. Biophys. Res. Commun.* **308**, 586–595 (2003).

70. Y. Geffen, E. Z. Ron, E. Rosenberg, Regulation of release of antibacterials from stressed scleractinian corals. *FEMS Microbiol. Lett.* **295**, 103–109 (2009).

71. D. A. Anderson, M. E. Walz, E. Weil, P. Tonellato, M. C. Smith, RNA-Seq of the Caribbean reef-building coral *Orbicella faveolata* (Scleractinia-Merulinidae) under bleaching and disease stress expands models of coral innate immunity. *PeerJ* **4**, e1616 (2016).

72. C. D. Kenkel, E. Meyer, M. V. Matz, Gene expression under chronic heat stress in populations of the mustard hill coral (*Porites astreoides*) from different thermal environments. *Mol. Ecol.* **22**, 4322–4334 (2013).

73. Z. Lipatova, N. Belogortseva, X. Q. Zhang, J. Kim, D. Taussig, N. Segev, Regulation of selective autophagy onset by a Ypt/Rab GTPase module. *Proc. Natl. Acad. Sci. U.S.A.* **109**, 6981–6986 (2012).

74. C. Kraft, F. Reggiori, M. Peter, Selective types of autophagy in yeast. *Biochim. Biophys. Acta* **1793**, 1404–1412 (2009).

Science Advances

Disease resistance in coral is mediated by distinct adaptive and plastic gene expression profiles

Nicholas J. MacKnight, Bradford A. Dimos, Kelsey M. Beavers, Erinn M. Muller, Marilyn E. Brandt, and Laura D. Mydlarz

View the article online
https://www.science.org/doi/10.1126/sciadv.abo6153
Permissions
https://www.science.org/help/reprints-and-permissions